

RELATING THE BREAKAGE INDEX AND SETTLEMENT OF GEOGRID-REINFORCED BALLAST

Chee-Ming Chan and Norsharina Abdul Rahman¹

¹Faculty of Engineering Technology, Universiti Tun Hussein Onn Malaysia, Malaysia

Abstract

Trains have historically served as a relatively economical, quick and safe mode of public and freight transportation. Rail tracks on which the trains traverse require regular maintenance to ensure optimum performance of the rail services. Often the track's superstructure seems to have received more attention than the substructure for performance assessment. As a foundation, the substructure, which is typically of ballast layer, plays the role of transferring the traffic load to the compacted subgrade. Degradation and breakage of ballast can lead to deformed track geometry and excessive or non-uniform track settlements, compromising the traffic ability and safety of the system. A potential approach to improve the performance of the ballast layer is geogrid reinforcement. The present study recreates the composite foundation in a lab-scale static test with geogrid placed at various heights in the ballast layer. The steel model box measured 200 mm x 200 mm x 200 mm. There was no apparent yielding of the ballast layer, with or without geogrid inclusion, indicative of a strain-hardening behaviour of the material under load. Taking the acceptable settlement as no more than 25 mm in a typical 300 mm ballast layer, the failure point was therefore defined at 8.3 % from the load-settlement curves. Sieve analysis was conducted on the ballast before and after the compression test to determine deterioration of the ballast via breakage under load. A graphical analytical method was next adopted to identify the Ballast Breakage Index (B_g) in relation to the overall settlement reduction. Overall particle breakage was not found to be expediently mitigated by geogrid installation in the ballast layer. The settlement reduction though was very much attributed to lateral spread control by the geogrid reinforcement.

Keywords: Ballasts, Geogrid, Compression, Settlement, Breakage Index

INTRODUCTION

Railway track is an important part of the transportation infrastructure and plays a significant role in sustaining a healthy economy. In the research of railway track systems, much attention has been given to the track superstructure but less so to the substructure [1]. This seeming unequal focus could be partially attributed to the difficulties in defining many variables of the substructure compared to those of the superstructure [2], potentially leading to safe but excessive designs. In general tracks should be designed to withstand large cyclic train loadings to provide protection to subgrade soils against both progressive shear failure and excessive plastic deformations [3]. Settlement or uneven track deterioration is the main cause of poor track geometry,

and this is highly dependent on individual site conditions, i.e. subgrade and ballast [4].

Being the main material in the rail track layer, ballast is understandably the primary contributor to track settlement problems (Fig. 1). Under traffic loading, ballast subjected to repeated and high stresses would undergo degradation and breakage, resulting in track deformation [5]. In addition, long term cyclic loading, excessive vibration, temperature and moisture variations as well as impact load on ballast can also lead to ballast degradation. Track maintenance using the tamping method is also known to contribute to ballast breakage [6]. Ballast degradation includes breakage of sharp edges, repeated grinding wear and crushing of weak particles, inevitable under the harsh working conditions and weathering effects. Therefore it is expedient to adopt innovative methods to improve the

serviceability and effectiveness of the rail tracks, such as with the inclusion of geogrid in ballast layer [4].

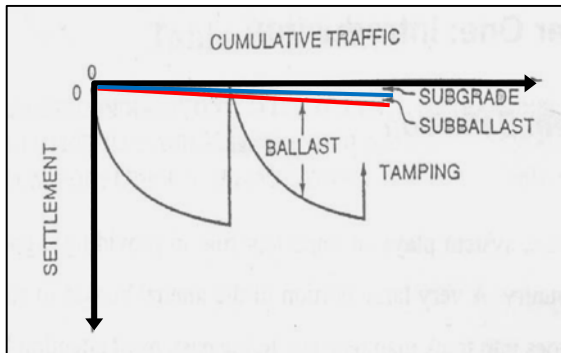


Fig. 1 Settlements due to substructure components [6]

In the present study, the potential of geogrid inclusion in the ballast layer for settlement reduction was investigated in a static compression test setup. The primary aim of the study was to relate the breakage index of the ballast with the overall settlement of the composite system.

EXPERIMENTAL SETUP

In this research, a lab-scale static compression test was conducted on the simulated ballast layer at a loading rate of 30 mm per minute (Fig. 2). The sample's load-vertical deformation was logged automatically at 20 data per minute. A steel model box measuring 200 mm x 200 mm x 200 mm was used to contain the material (Fig. 3). The box was filled with well-graded ballast of size ranging from 10 to 50 mm. Note that the steel model box was lined with 10 mm thick foam to minimize the confining effect of the otherwise hard walls and base. A custom made plunger-loading plate was used to transfer the load uniformly onto the sample (Fig. 3).

The sample was prepared in layers, where each layer was initially placed loose at approximately 60 mm thick. Each layer was next subjected to 25 times of steel rod tamping. Apart from the Control sample, every sample had geogrid installed at depths of 50, 90 or 130 mm from the top of the sample. It is also important to note that in order for the geogrid (TenCate GX60/30) to function accordingly in the setup, it was cut out slightly oversize with a small fold-over of 5 mm on each side of the foamed walls (Fig. 4).

3 different loads were applied during the tests, i.e. 1.0, 1.5 and 3.0 MPa to monitor degradation of the ballast with different load applications. The ballast layer was considered to have failed in terms of

settlement or vertical deformation when it exceeded 8.3 %, which corresponds with 25 mm in a typical 300 mm thick ballast layer on site. Sieve analysis was carried out on each sample post-test to ascertain the amount of breakage that took place under the respective loads.

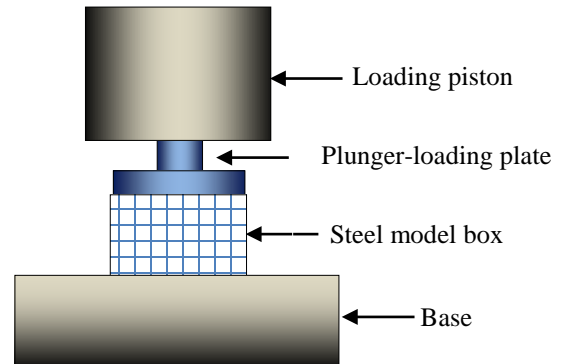


Fig. 2 Schematic diagram of compression test setup

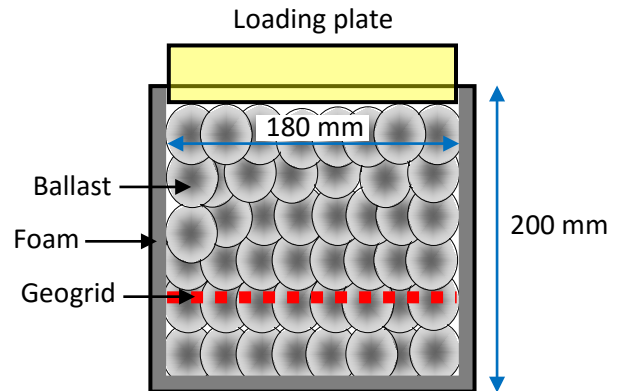


Fig. 3 Configuration of simulated ballast layer with geogrid reinforcement (side view)



Fig. 4 Geogrid overlying a compacted ballast layer

The severity of ballast breakage was determined by referring to the Ballast Breakage Index (B_g). The pre- and post-test sieve analysis curves of the ballast were combined to form a chart as shown in Fig. 5. By adopting the graphical derivation proposed by Indraratna & Salim [7], the ballast degradation level can be determined via the B_g value. However, a slight modification of the method was made by drawing a straight line connecting the origin with the intersection of the pre- and post-test curves (Fig. 5). The area enclosed by the straight line and the post-test curve is termed A_f , while the area bound by the post-test curve and the lower lying pre-test curve is termed A_i . Equation (1) is then used for the B_g calculation.

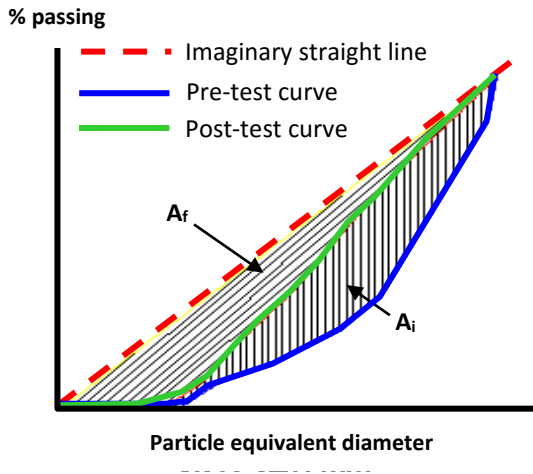


Fig. 5 Graphical derivation for B_g calculations

$$B_g = \frac{A_i}{A_f + A_i} \quad (1)$$

RESULTS AND DISCUSSIONS

Settlement

Fig. 6 shows settlement (in terms of vertical strain) plotted against the applied stresses of 1.0, 1.5 and 3.0 MPa respectively. The data were grouped according to the depth of geogrid embedment, D_g .

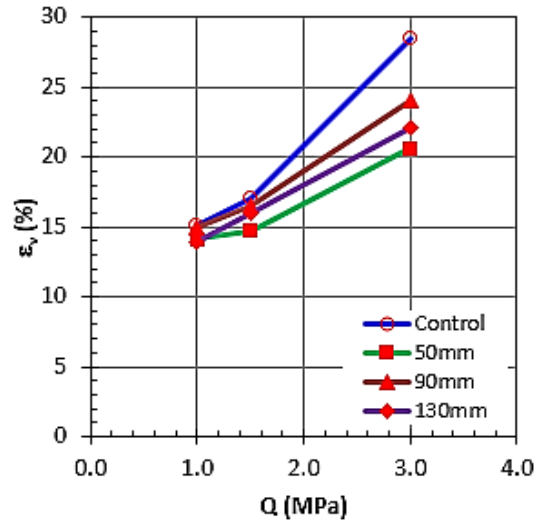


Fig. 6 Vertical strain (ϵ_v) – applied stress (Q)

It is apparent that settlement increased with loading irrespective of the geogrid reinforcement, though the relationship does not appear to be linear. The rate of vertical displacement was more pronounced beyond 1.5 MPa, as indicated by the steeper rise in gradient of the plots. Nonetheless the rather parallel plots suggest similar settlement rate but at different magnitude, as expected with increased applied stresses on the sample. This could be attributed to either breakage of the aggregates and lateral spread of the simulated ballast mass, but both mechanisms do not necessarily take place simultaneously when geogrid is sandwiched in the ballast layer. Without reinforcement, the recorded settlement was the largest, i.e. Control sample. The embedment depth of the geogrid had a significant effect on the resulting reduced settlement. Intuitively the stiffening effect of the geogrid would diminish with greater D_g as the geogrid was installed deeper in the ballast layer and away from the point of load application. This was true for sample $D_g = 50$ mm but the plots in Fig.6 also show that the sample with geogrid embedment at 130 mm outperformed that with $D_g = 90$ mm. Discourse about this seeming discrepancy is made in later sections in conjunction with the particle breakage phenomenon.

In addition to particle breakage and lateral spread, a third possibility causing settlement in a reinforced system could be found at the geogrid-ballast interface zone [1]. Considering that interlocking with the geogrid and among the particles are best achieved with a good granular material mix, the 'too large' or 'too small' ballast or aggregates could actually bring forth adverse effect. The

displacement, though minute, could be sizable when taken in accumulation. At the geogrid-ballast interface, the larger aggregates (≥ 24 mm) exerting localized stresses on the geogrid, which aperture, measuring 24 x 24 mm, was relatively smaller. Also possible was small localized subsidence caused by the smaller aggregates (< 24 mm) being pushed through the aperture instead of interlocking with the geogrid. Fig. 7 illustrates these 2 possible individual aggregate-geogrid interactions that could contribute to the overall settlement measured. This phenomenon suggests the important role played by aggregates at the geogrid-ballast interface: to ensure affective gripping and interlocking for improved load-bearing, perhaps only selectively sieved material are spread over the geogrid to avoid the adverse effects discussed above [4].

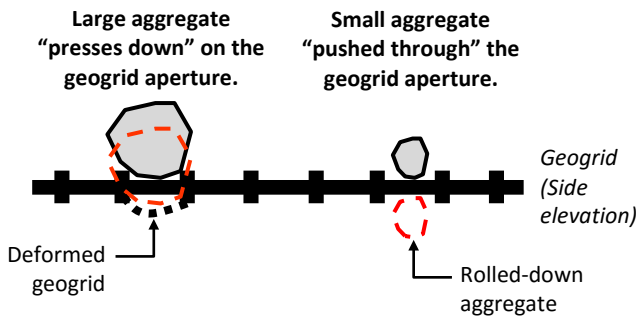


Fig. 7 Interaction of individual aggregates at the geogrid interface.

The overall settlement or vertical strain (ϵ_v) – geogrid embedment depth (D_g) plots are shown in Fig. 8. As expected, the settlement increased with greater applied stress in all samples, regardless of the presence of geogrid or not. However the immediate reduction in settlement with geogrid reinforcement was obvious, as demonstrated by the generally declining plots for all samples. Note that settlement reduction was especially significant at higher stresses, evident in the steep drop in ϵ_v for sample 3.0 MPa. This indicates the greater frictional resistance mobilized within the ballast layer when subjected to higher loads, resulting in better load-bearing capacity and effective subsidence control. Samples 1.0 and 1.5 MPa showed negligible differences in terms of the ϵ_v recorded, most probably due to the rather small difference in the loading magnitude itself. In comparison with sample 3.0 MPa, which was loaded up to twice or more that of the other 2 samples, the settlement reduction at $D_g = 50$ mm was close to 40 %.

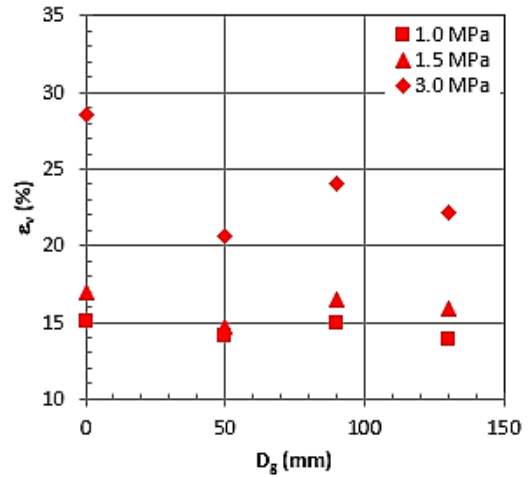


Fig. 8 Vertical strain (ϵ_v) – geogrid embedment depth

Interestingly, magnitude of the settlement aside, the settlement control plots seemed to follow a similar pattern among the different samples, i.e. the most significant drop in settlement at $D_g = 50$ mm, followed by a slight rise at $D_g = 90$ mm and small decline at $D_g = 130$ mm. In corroboration with the settlement control patterns afforded by geogrid reinforcement observed in Fig. 6, $D_g = 90$ mm produced the least satisfactory results for all stresses applied. The uncannily similar trends of the plots in Fig. 8 point to a possible common behaviour shared by all samples, which explains the greater settlement recorded when geogrid was placed at mid-height than near the base ($D_g = 130$ mm) of the sample.

Particle Breakage

As mentioned earlier, the Ballast Breakage Index (B_g) is calculated based on the area covered by the particle size distribution curves before and after the test, i.e. A_i and A_f (Fig. 9). The 1:1 dashed line represents uniformity between A_i and A_f . It was found that $A_i = 20.5 - A_f$ in this particular case, suggesting changes in the particle size composition of the simulated ballast post-compression tests. Fig. 10 compiled the $B_g - Q$ plots for all samples. In comparison with the Control sample, the presence of geogrid clearly reduced particle breakage. Settlement reduction at the highest load was between 40 to 150 %. The amount of particle breakage was very similar for the $D_g = 90$ and 130 mm samples at 1.0 MPa, suggesting the need for greater applied stresses to mobilize frictional resistance between the simulated ballast and geogrid. In fact, load increment to 1.5 MPa was still inadequate to initiate the

geogrid's functional resistance in the $D_g = 90$ mm sample.

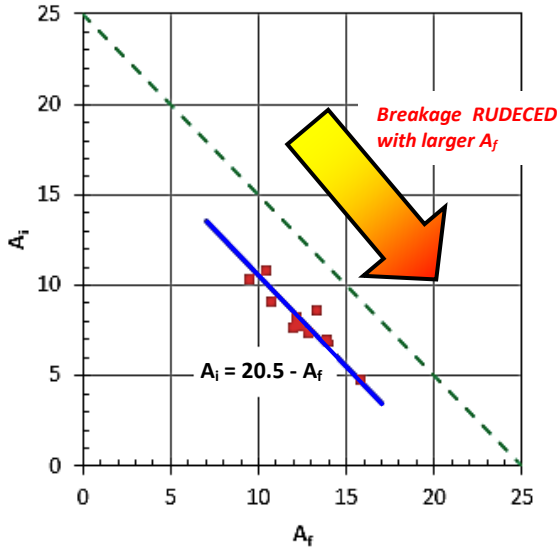


Fig. 9 Initial curve area ratio (A_i) – final curve area ratio (A_f)

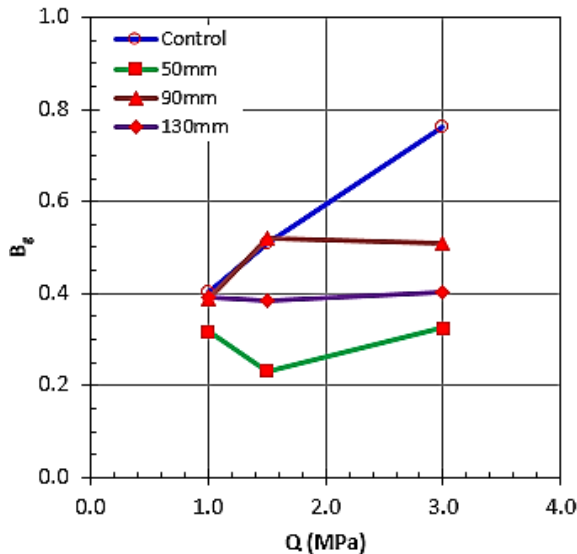


Fig. 10 Breakage Index (B_g) – applied stress (Q)

Note that the $D_g = 90$ mm sample was outperformed by $D_g = 130$ mm in terms of B_g reduction, with its plot lying consistently above that of $D_g = 130$ mm except beyond 1.0 MPa. Indeed the $D_g = 130$ mm sample showed negligible changes in B_g , with apparent insensitivity towards load increment. Closer inspection revealed unchanged B_g values from 1.0 MPa load application, i.e. the same

amount of breakage as with the sample without geogrid reinforcement (Control). Under these circumstances, the resulting settlement would not have been caused by failure of the individual particles which broke into smaller fragments under load. It follows that the settlement observed can only be attributed to lateral spread instead, where the geogrid inclusion somehow failed to prevent horizontal movement of the simulated ballast during load transfer.

This could be the explanation to the puzzling findings as discussed earlier with reference to Fig. 6 and 8, where settlement control was less effective when the geogrid was installed at mid-height ($D_g = 90$ mm) than near the base of the sample ($D_g = 130$ mm). It is reasoned that the resulting settlement is not attributed to the particle breakage but lateral spread, the other factor that contributes to settlement in a geogrid reinforced granular mass. Placement of the geogrid at $D_g = 130$ mm provided minimal load resistance for the simulated 180 mm thick ballast layer, causing the material above the geogrid to expand laterally when loaded. This was however, not accompanied by significant particle breakage as the load was transferred rather uniformly through the overlying ballast to the reinforced plane, as demonstrated by the generally constant B_g in Fig. 10. In other words, the consequence of lateral spread was more dominant than that of particle breakage for sample $D_g = 130$ mm in settlement of the ballast layer; whereas in the case of sample $D_g = 90$ mm, between 1.5 and 3.0 MPa, the effect of lateral spread overshadowed that of particle breakage in the resulting settlement.

On the other hand, the $D_g = 90$ mm sample recorded higher settlement (see Fig. 6 & 8) due to both particle breakage as well as lateral spread, hence the apparent compromised effectiveness of geogrid placement at a shallower depth in the ballast. Indeed, taking into account the relatively unchanged B_g for $D_g = 90$ mm sample between 1.5-3.0 MPa (Fig. 10), the resulting increased settlement with increased load would have been mainly caused by lateral spread and not particle breakage. These observations highlight the crucial role of geogrid installation depth for effective particle breakage resistance.

Relating Settlement and Particle Breakage

Fig. 11 relates vertical strain (ϵ_v) and the Ballast Breakage Index (B_g). The outlying data point (circled) is that of the Control sample subjected to 3.0 MPa. The corresponding moderate B_g value indicates that the high settlement was not predominated by particle breakage. Overall larger settlements took place with higher B_g values, i.e. more significant

particle breakage occurrence. Note the comparatively milder rise in the ϵ_v - B_g plots for $Q < 3.0$ MPa with very close settlement measurements, suggesting the negligible effect particle breakage had on the overall vertical deformation of the ballast layer. Taking into the plot for $Q = 3.0$ MPa, in spite of the common range of B_g for all cases, i.e. 0.23-0.53, the settlement encompassed a wide range between 14 and 24 %. This corroborates with earlier discourse and Fig. 5 that the overall settlement was attributed mainly to lateral spread alone.

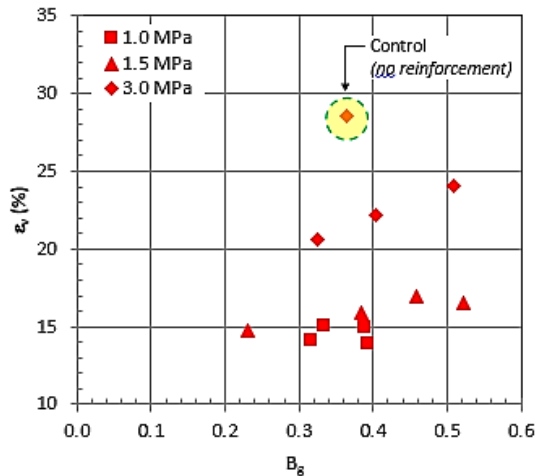


Fig. 11 Vertical strain (ϵ_v) – Breakage Index (B_g)

CONCLUSION

Settlement is generally reduced with geogrid installation, with better reinforcement provided by smaller embedment depth, B_g . Ballast in direct contact with the geogrid at the interface could potentially affect the overall settlement reduction due to either the ‘pressed-down’ or ‘pushed through’ phenomenon, attributed to poorly selected ballast sizes relative to the geogrid aperture. While settlement increased with loading, the effectiveness of geogrid was especially pronounced when $D_g = 50$ mm in all cases. Breakage of the simulated ballast was evident in the A_f - A_f plots, from which the Ballast Breakage Index (B_g) was derived. All samples with geogrid reinforcement were found to undergo less particle breakage, with $D_g = 50$ mm giving the best results, i.e. 150 % reduction in particle breakage. Interestingly, the $D_g = 130$ mm sample showed almost no changes in B_g despite the increased loading: load transfer took place without breakage of the simulated ballast. Therefore the resulting settlement was not caused by particle breakage but lateral spread alone. In a nutshell, the placement

depth of geogrid clearly influences settlement control of the ballast layer, primarily by way of minimizing the lateral spread under load. The incorporation of geogrid in the ballast layer was not found to be particularly effective in particle breakage reduction, more so in cases with greater applied loads.

ACKNOWLEDGEMENT

The geogrid was sponsored by TenCate Geosynthetics Asia Sdn. Bhd. and funds for the study were made available via the LEP2.0 research grant by MOHE, Malaysia.

REFERENCES

- [1] Wee, L.L. “Mechanics of Railway Ballast Behaviour”, 2014. The University of Nottingham. Thesis Degree of Philosophy.
- [2] Said, D. Xie, G. & Liu X. “Equivalent Dynamics Model of Ballasted Track Bed”, 2012. Department of Mechanical Engineering Blekinge Institute of Technology Karlskrona, Sweden.
- [3] Indraratna, B. “Implications of Ballast Breakage on Ballasted Railway Track based on Numerical Modelling”, 2011. Faculty of Engineering and Information Sciences, University of Wollongong.
- [4] Ching, C.J.K. “Geogrid Reinforcement of Railway”, 2006. The University of Nottingham. Thesis Degree of Philosophy.
- [5] Indraratna, B., Shahin, M.A. & Rujikiatkamjorn, C. “Stabilisation of Rail Tracks and Underlying Soft Soil Formations”, 2006. Faculty of Engineering and Information Sciences, University of Wollongong.
- [6] Selig, E.T. & Waters J.W. “Track Geotechnology and Substructure Management”, 1994. Thomas Telford Publishers, London, UK.
- [7] Indraratna, B. & Salim, W. “Mechanics of Ballasted Rail Tracks: A geotechnical Perspective”, 2005. Taylor & Francis, London, UK.

Int. J. of GEOMATE, Feb., 2016, Vol. 10, No. 1 (Sl. No. 19), pp. 1687-1692.

MS No.150801 received on Aug. 1, 2015 and reviewed under GEOMATE publication policies. Copyright © 2016, International Journal of GEOMATE. All rights reserved, including the making of copies unless permission is obtained from the copyright proprietors. Pertinent discussion including authors’ closure, if any, will be published in Feb. 2017 if the discussion is received by Aug. 2016.

Corresponding Author: **Chee-Ming Chan**